

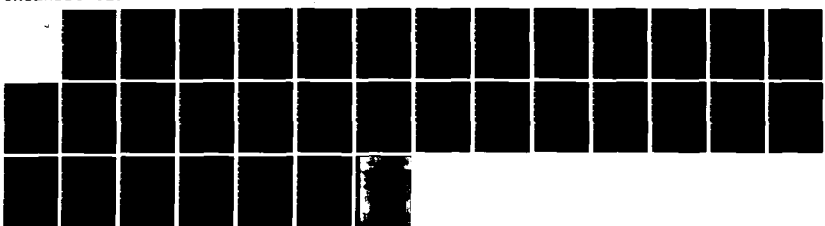
RD-A142 439

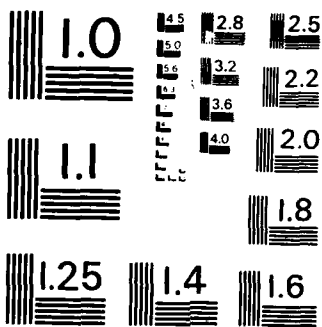
SURFACE-ENHANCED RAMAN SPECTROSCOPY OF
PENTRAMMINEOSMUM(III)/(II) AND PE. (U) PURDUE UNIV
LAFAYETTE IN DEPT OF CHEMISTRY S FARQUHARSON ET AL
UNCLASSIFIED APR 84 TR-28 N80014-79-C-0670

1/1

F/G 7/4

NL





MICROCOPY RESOLUTION TEST CHART
NATIONAL BUREAU OF STANDARDS 1963-A

AD-A142 439

DTIC FILE COPY

OFFICE OF NAVAL RESEARCH

Contract N00014-79-0670

TECHNICAL REPORT NO. 28

Surface-Enhanced Raman Spectroscopy of Pentaammineosmium(III)/(II) and Pentaammineruthenium(II) Containing Pyridine, Pyrazine, or 4,4'-Bipyridine Ligands at Silver Electrodes: Vibrational Assignments

by

Stuart Farquharson, Peter A. Lay, and Michael J. Weaver

Prepared for Publication

in the

Spectrochim. Acta A.

Department of Chemistry

Purdue University

West Lafayette, IN 47907

April 1983

Reproduction in whole or in part is permitted for
any purpose of the United States Government

This document has been approved for public release
and sale; its distribution is unlimited

84 06 26 003

REPORT DOCUMENTATION PAGE		READ INSTRUCTIONS BEFORE COMPLETING FORM
1. REPORT NUMBER	2. GOVT ACCESSION NO.	3. RECIPIENT'S CATALOG NUMBER
Technical Report No. 28	AD-A142439	
4. TITLE (and Subtitle)	5. TYPE OF REPORT & PERIOD COVERED	
Surface-Enhanced Raman Spectroscopy of Pentaammineosmium(III)/(II) and Pentaammineruthenium(II) Containing Pyridine, Pyrazine, or 4,4'-Bipyridine Ligands at Silver Electrodes: Vibrational Assignments	Technical Report No. 28	
7. AUTHOR(s)	6. PERFORMING ORG. REPORT NUMBER	
Stuart Farquharson, Peter A. Lay, Michael J. Weaver	8. CONTRACT OR GRANT NUMBER(s)	
	N00014-79-0670	
9. PERFORMING ORGANIZATION NAME AND ADDRESS	10. PROGRAM ELEMENT, PROJECT, TASK AREA & WORK UNIT NUMBERS	
Department of Chemistry Purdue University West Lafayette, IN 47907		
11. CONTROLLING OFFICE NAME AND ADDRESS	12. REPORT DATE	
Office of Naval Research Department of the Navy Arlington, VA 22217	April 1984	
14. MONITORING AGENCY NAME & ADDRESS (if different from Controlling Office)	13. NUMBER OF PAGES	
	15. SECURITY CLASS. (of this report)	
	Unclassified	
16. DISTRIBUTION STATEMENT (of this Report)	15a. DECLASSIFICATION/DOWNGRADING SCHEDULE	
Approved for public release; distribution unlimited		
17. DISTRIBUTION STATEMENT (of the abstract entered in Block 20, if different from Report)		
18. SUPPLEMENTARY NOTES		
19. KEY WORDS (Continue on reverse side if necessary and identify by block number)		
vibrational assignments, Raman and infrared spectra, SER spectra		
20. ABSTRACT (Continue on reverse side if necessary and identify by block number)		
Detailed vibrational assignments are described for Surface Enhanced Raman (SER) spectra of pentaammineosmium(III), (II) and pentaammineruthenium(II) containing pyridine (py), pyrazine (pz), and 4,4'-bipyridine (bpy) ligands adsorbed at the silver-aqueous interface. The assignments are based on group symmetry analysis, deuteration effects, and by comparison with corresponding normal Raman and infrared spectra for the solid-phase complexes and surface and bulk Raman spectra for the corresponding free ligands. Most bands present in the normal Raman and/or infrared spectra also appear in the SER spectra. This		

results from the high intensity of the SER spectra along with the relaxation of vibrational selection rules for adsorbed molecules. The appearance of intense SER spectra for $\text{Os}(\text{NH}_3)_5\text{py(III)/(II)}$ and $\text{Ru}^{\text{II}}(\text{NH}_3)_5\text{py}$ is noteworthy since unlike free pyridine, these lack an available nitrogen for surface coordination. The results illustrate the virtues of electrochemical SER spectroscopy for examining the detailed vibrational properties of coordination compounds, including those in oxidation states (such as Os(II) here) that are difficult to obtain pure in bulk media.

Accession For	
NTIS GRA&I	<input checked="" type="checkbox"/>
DTIC TAB	<input type="checkbox"/>
Unannounced	<input type="checkbox"/>
Justification	
By _____	
Distribution/	
Availability Codes	
ARPA/NSF/DOE/	<input type="checkbox"/>
Dist	Special
A-1	



SURFACE-ENHANCED RAMAN SPECTROSCOPY OF PENTAAMMINEOSMIUM(III)/(II) AND
PENTAAMMINERUTHENIUM(II) CONTAINING PYRIDINE, PYRAZINE, OR 4,4'-
BIPYRIDINE LIGANDS AT SILVER ELECTRODES: VIBRATIONAL ASSIGNMENTS

Stuart Farquharson, Peter A. Lay[†], and Michael J. Weaver*

Department of Chemistry, Purdue University, West Lafayette, Indiana 47907

ABSTRACT

Detailed vibrational assignments are described for Surface Enhanced Raman (SER) spectra of pentaammineosmium(III), (II) and pentaammineruthenium(II) containing pyridine (py), pyrazine (pz), and 4,4'-bipyridine (bpy) ligands adsorbed at the silver-aqueous interface. The assignments are based on group symmetry analysis, deuteration effects, and by comparison with corresponding normal Raman and infrared spectra for the solid-phase complexes and surface and bulk Raman spectra for the corresponding free ligands. Most bands present in the normal Raman and/or infrared spectra also appear in the SER spectra. This results from the high intensity of the SER spectra along with the relaxation of vibrational selection rules for adsorbed molecules. The appearance of intense SER spectra for $\text{Os}(\text{NH}_3)_5\text{py(III)/(II)}$ and $\text{Ru}^{\text{II}}(\text{NH}_3)_5\text{py}$ is noteworthy since unlike free pyridine, these lack an available nitrogen for surface coordination. The results illustrate the virtues of electrochemical SER spectroscopy for examining the detailed vibrational properties of coordination compounds, including those in oxidation states (such as Os(II) here) that are difficult to obtain pure in bulk media.

[†] Department of Chemistry, Stanford University, Stanford, CA 94305.
Present address: Division of Applied Organic Chemistry, CSIRO, G.P.O. Box 4331, Melbourne, Victoria 3001, Australia

*Author to whom correspondence should be addressed.

INTRODUCTION

Although only in its infancy surface-enhanced Raman spectroscopy (SERS) has been demonstrated to be a valuable tool for gaining detailed structural information for molecules adsorbed at metal surfaces.¹ Preliminary investigations have demonstrated that a variety of adsorbates can be detected, from simple halide and pseudohalide anions^{2,3} to complex molecules such as cytochrome c.⁴ It also appears that the SERS effect may be limited to a select group of metal surfaces, most prominently silver, copper and gold.¹ Although a large proportion of SERS investigations have been aimed at elucidating the mechanism responsible for the unexpected signal enhancement, several practical applications are beginning to emerge. Thus SERS has yielded information on the nature of adsorbate-electrode bonding, and the alterations brought about by variations in electrode potential.^{3,5} Also, recent studies indicate that under favorable conditions the Raman intensities are approximately proportional to adsorbate coverage.⁶

SERS studies are also starting to appear on adsorbates that undergo electrochemical reactions.⁷⁻¹¹ We have recently demonstrated that SERS can be utilized to follow heterogeneous electron transfer for several adsorbed redox couples,^{8,9} including pentaamminepyridineosmium(III)/(II) and pentaamminepyrazineosmium(III)/(II), at the silver-aqueous interface.⁸ These and related pentaammineosmium and pentaammineruthenium complexes containing nitrogen heterocycles are of particular interest since they form structurally simple transition-metal complexes that are substitutionally inert in both III and II metal oxidation states.⁸ We have made quantitative comparisons of the potential-dependent SER spectra with the redox thermodynamics of these electroactive adsorbates obtained using conventional electrochemical techniques.^{8b}

The present communication contains detailed vibrational analyses of SER spectra for $\text{Os}(\text{NH}_3)_5\text{Py(III)/(II)}$ [py = pyridine], $\text{Os}(\text{NH}_3)_5\text{pz(III)/(II)}$ [pz = pyrazine], $\text{Os}(\text{NH}_3)_5\text{bpy(III)/(II)}$ [bpy = 4,4'-bipyridine], $\text{Ru}^{\text{II}}(\text{NH}_3)_5\text{py}$, and $\text{Ru}^{\text{II}}(\text{NH}_3)_5\text{pz}$. Vibrational mode assignments are based on group symmetry considerations, combined with the frequency shifts observed upon selective deuteration, and comparison with corresponding bulk-phase normal Raman and Infrared spectra for these and related nitrogen heterocycle compounds. This report of the spectral details complements the comparisons of the potential-dependent spectral features with the electrochemical redox behavior of the complexes given in ref. 8b.

Although the silver electrode does perturb the vibrational properties of these adsorbates, the extent is small, especially for the pyridine adsorbates which lack an additional nitrogen for surface binding. The most detailed spectra data were gathered for $\text{Os}(\text{NH}_3)_5\text{py(III)/(II)}$ for which the most well-defined change in redox state from Os(III) to Os(II) is apparent upon altering the potential to more negative values.⁸ Besides the remarkable intensity and richness of the SER spectra, some of these results demonstrate the virtue of the electrochemical SERS technique for obtaining detailed vibrational information for coordination compounds in very dilute solutions that are difficult or even impossible to observe by means of bulk-phase Raman or infrared measurements.

EXPERIMENTAL

The $\text{Os}^{\text{III}}(\text{NH}_3)_5\text{py}$, $\text{Os}^{\text{III}}(\text{NH}_3)_5\text{pz}$ and $\text{Os}^{\text{III}}(\text{NH}_3)_5\text{bpy}$ complexes were prepared as trifluoromethanesulfonate or halide salts as detailed in ref. 12a, and the corresponding Ru^{III} and Ru^{II} complexes as in ref. 12b. The SER spectra were obtained for 0.05 - 1 mM aqueous solutions of these complexes in either 0.1 M NaCl or NaBr . For the pyridine complexes, 0.1 M HCl was added in order to

suppress base-catalyzed disproportionation.¹³ Other relevant details are given in ref. 8b.

The SERS electrochemical cell consisted of a cylindrical glass container with an optical flat base through which the laser beam was focussed on to the silver surface.¹⁴ This electrode was of rotating disk construction, having an exposed face of diameter 0.4 cm, encased in a Teflon shroud. It was mechanically polished successively with 0.1 μ and 0.3 μ alumina immediately before immersion in the cell, and then electrochemically roughened in order to optimise the SERS intensities by means of an oxidation-reduction cycle (ORC) in the conventional manner.^{1a,8b} The cell also contained an isolated silver-silver chloride or saturated calomel reference electrode, a platinum wire counter electrode, and an argon inlet tube for purging the solution.

Raman excitation was obtained using either a Spectra Physics Model 165 Kr⁺ laser (647.1 nm) or Ar⁺ laser (514.5 nm). The laser beam of 100 mW intensity was spot focussed at an incident angle of 60° to the electrode surface. The Raman scattering was collected at 90° to the surface, and focussed into a Jarrell-Ash Model 25/100 scanning double monochromator. The spectral resolution was ca. 4 cm⁻¹. The signal was detected with an RCA C31034 photomultiplier tube, amplified by a Victorean Model CTE-1 micro-microammeter, and displayed on a Hewlett-Packard Model 7100 strip chart recorder using a 1 cm sec⁻¹ scanning rate and a 1 sec time constant. All spectra were frequency calibrated using laser plasma emission lines. Normal Raman and Fourier transform infrared spectra of the complexes were recorded as solid samples in KBr or CsI pellets. The former employed a rotating wheel to minimize photodecomposition. The latter were obtained using a Nicolet Model 7194 FTIR spectrometer.

Electrode potentials are quoted versus the saturated calomel electrode (sce). All experiments were conducted at $23 \pm 1^\circ\text{C}$.

RESULTS AND DISCUSSION

Listings of the various surface-enhanced Raman (SER), normal Raman (NR), and infrared (IR) vibrational bands seen for each complex are given in Tables 1-5. SER spectra for the complexes are given for a representative pair of electrode potentials in order to provide a basic summary of the potential-induced spectral changes. For $\text{Os}(\text{NH}_3)_5\text{py}$, $\text{Ru}(\text{NH}_3)_5\text{py}$, and $\text{Os}(\text{NH}_3)_5\text{pz}$ (Table 1, 2, and 3, respectively) normal Raman and/or infrared data are given for both III and II metal oxidation states. For the first complex, the SER spectra obtained at -150 mV. vs sce are consistent with $\text{Os}^{\text{III}}(\text{NH}_3)_5\text{py}$ on the basis of frequency comparisons with the corresponding normal Raman spectrum, whereas that obtained at -750 mV corresponds to $\text{Os}^{\text{II}}(\text{NH}_3)_5\text{py}$.⁸ On the other hand, the SER spectra for $\text{Ru}(\text{NH}_3)_5\text{py}$ and $\text{Ru}(\text{NH}_3)_5\text{pz}$ are consistent with the presence of Ru(II) throughout the observable potential region negative of ca -100 mV. at silver electrodes.⁸ [The surface $\text{Os}(\text{III})/(\text{II})$ formal potential, E_a^f , equals -670 mV.^{8b}] Similarly, a number of potential-induced changes in the $\text{Os}(\text{NH}_3)_5\text{pz}$ SER spectra are consistent with reduction of Os(III) to Os(II) ($E_a^f = -310$ mV^{8b}), although for this complex as well as for $\text{Os}(\text{NH}_3)_5\text{bpy}$ these changes do not appear to be associated simply with electroreduction of Os(III) to Os(II).^{8b} (For simplicity the osmium and ruthenium oxidation states associated with particular vibrational modes will not be designated except where they are clear cut and/or the frequencies are sensitive to the oxidation state). For $\text{Os}^{\text{III}}(\text{NH}_3)_5\text{py}$ and $\text{Os}^{\text{II}}(\text{NH}_3)_5\text{py}$, SER frequencies are also given for samples where the pyridine ring or the ammine ligands were separately deuterated (Table 1).

Nearly all of the observed vibrational bands listed for these complexes in Table 1-5 can be accounted for in terms of metal-ligand, ammine, or nitrogen heterocycle modes. Included in these Tables along with the vibrational assignments are the associated symmetry species as well as a brief description. Following

standard nomenclature the stretching modes are designated ν , the in-plane bending modes δ , the out-of-plane bending modes γ , and the rocking modes ρ . The nitrogen heterocycle bands are additionally given Wilson mode numbers in accordance with established procedure.¹⁵

Metal-ligand modes.

The vibrational mode assignments are well established for transition-metal hexaammines¹⁶ and for several pentaammine complexes.¹⁷ For such pentaammine complexes with C_{4v} symmetry there are fifteen predicted metal-ligand vibrations; $4A_1$, $2B_1$, $1B_2$ and $4E$ symmetry species. (Note that only eleven unique modes result since the E modes are doubly degenerate.¹⁸) All of these modes are Raman active, whereas only the totally symmetric A_1 and the degenerate E modes are IR active. These modes are generally observed between 250 and 600 cm^{-1} .^{17,19} In the present spectra as many as nine modes are observed in this spectral region. This compares favorably to the normal Raman spectra of metal halopentaammines which yield only four to seven observable peaks.¹⁷ Similarly, at most three IR and two normal Raman peaks in this frequency region are observed for the present complexes (Tables I-IV). The absence of further peaks is presumably due to low signal intensities and accidental degeneracies. In addition to the modes given in Tables I-IV, the SER spectra also contain a low frequency band attributed to a silver surface-halide stretching mode from either the bromide or chloride ions used as the supporting electrolyte.²⁰ The presence of these anions is desirable for the production of stable intense SER spectra following the ORC.^{8b} These surface-halide bands are easily identified by a frequency shift from around 240 to 180 cm^{-1} that occurs upon the substitution of bromide for chloride anions;²⁰ the SER spectra for the present complexes are otherwise unchanged.^{8b}

The most interesting and indeed prominent band in the low frequency region of the SER spectra occurs around 300 cm^{-1} , and is attributed to a metal-nitrogen

heterocycle stretching mode, I (the metal-ligand modes are labelled with Roman numerals, see Tables 1-5). The unexpectedly high intensity of this mode may be attributable to interaction between the heterocycle with the electrode surface, via physical (or electrostatic) adsorption as in the case of the pyridine complexes and possibly via chemisorption of the remote nitrogen for the pyrazine and bipyridine complexes. Indeed, the greater surface-heterocycle interaction expected with the latter adsorbates may well be related to the particular intensity of this and the other SERS bands with these systems.^{8b}

The band at 267 cm^{-1} seen for $\text{Os}(\text{NH}_3)_5\text{py}$ at -750 mV is ascribed to $\text{Os}(\text{II})$ -pyridine stretching. Although a very weak band at 291 cm^{-1} appearing at less negative potentials was originally ascribed to an $\text{Os}(\text{III})$ -pyridine vibration,^{8a} this assignment is probably incorrect.^{8b} For the pyrazine complexes, mode I is tentatively assigned to the band that occurs between 300 and 350 cm^{-1} (Tables 3 and 4). The appearance of a band at 304 cm^{-1} at more negative potentials for $\text{Os}(\text{NH}_3)_5\text{pz}$ may be associated with the $\text{Os}(\text{II})$ complex. However, these potential-dependent changes do not appear to be associated with a simple adsorbed redox couple since the higher frequency band (345 cm^{-1}) persists even at negative potentials (Table 3).^{8b} A puzzling feature is the surprisingly high frequencies at which these bands appear for the pyrazine complexes: metal-pyrazine stretching modes are typically observed for divalent pyrazine complexes at ca. 250 - 280 cm^{-1} .²² The present higher frequencies may arise from surface binding of the pyrazine ligand. Peaks around 300 - 330 cm^{-1} , ascribed to metal-pyrazine stretching, can also be seen for binuclear metal complexes containing pentaamminepyrazineruthenium(II).^{23,24} The strong SER bands seen at 370 - 400 cm^{-1} for $\text{Os}(\text{NH}_3)_5\text{bpy}$ (Table V) are also somewhat puzzling in this regard. However, intense modes at similar frequencies have also been observed for $\text{Ru}^{II}(2,2'\text{-bipyridine})(\text{py})_4$ both at silver electrodes and in bulk media.²⁵

The metal-ammine modes are expected to shift to lower frequencies by a factor of 0.92 upon deuteration of the ammine modes on the basis of the square root of the ligand mass ratio $(17/20)^{1/2}$. Such deuteration effects were examined for SERS of $\text{Os}(\text{NH}_3)_5\text{py}(\text{III})/(\text{II})$ for which the most well-defined metal-ammine modes were observed (Table 1). Precisely such a shift occurs for the $\text{Os}^{\text{III}}(\text{NH}_3)_5\text{py}$ band at 494 cm^{-1} and the $\text{Os}^{\text{II}}(\text{NH}_3)_5\text{py}$ band at 468 cm^{-1} . Although these bands also exhibit small decreases upon deuteration of the pyridine ligand (Table 1), these shifts can be rationalized in terms of coupling between the metal-ammine and metal-pyridine modes. Such coupling is anticipated for E symmetry metal-ammine modes.¹⁷

The band around 415 cm^{-1} for $\text{Os}(\text{NH}_3)_5\text{py}$ is most likely due to a pyridine ring mode (vide infra). Although several other SERS bands occur in the frequency region $400-550 \text{ cm}^{-1}$ for the various complexes which are probably due to other metal-ammine modes, unambiguous assignments are lacking in some cases (Tables 1-5). A difficulty with the pyrazine complexes is that most metal-ligand modes are dwarfed by the intensity and breadth of the metal-pyrazine modes noted above. Several of these modes are nonetheless observed in the IR and Raman spectra and are assigned according to their expected activity from selection rules (Tables 3 and 4).

Internal Ammine Modes

All five internal ammine vibrational modes expected are commonly observed as strong bands in the IR spectra for metal ammine complexes.^{16,19} Of these, SERS bands at 3200 , 1620 , and 1350 cm^{-1} are observed for $\text{Os}^{\text{III}}(\text{NH}_3)_5\text{py}$ which can be ascribed to N-H stretching, and asymmetric and symmetric NH_3 bending, respectively (Table 1). The last-named mode is of particular interest as its frequency decreases about 100 cm^{-1} , from 1354 to 1254 cm^{-1} , upon reduction of $\text{Os}(\text{III})$ to $\text{Os}(\text{II})$ (Table 1). Such a strong sensitivity of this band to the nature of the coordinated metal, including the metal oxidation state, has been noted

previously.¹⁶ This assignment is also supported by the large deuterium isotope effect observed for this mode (Table 1). The assignment for the 1620 cm^{-1} band is also supported by the substantial frequency decrease seen upon deuterium isotope substitution (Table 1). However, the band at 3200 cm^{-1} appears to be complicated by accidental degeneracy with the C-H stretching modes also expected in this region (Table 1). Several of these modes also appear in the SER spectra for the other complexes, although they are probably obscured in some cases by the more intense heterocycle ring modes. The ammine rocking mode is observed in the SER spectra for $\text{Ru}(\text{NH}_3)_5\text{py}$, nearly coincident in frequency to its IR value of 815 cm^{-1} (Table 2).

It should be noted that the appearance of metal-ammine and internal ammine modes in the SER spectra is in itself noteworthy since the ammine ligands are not expected to interact with, and may well be relatively remote from, the metal surface. Nevertheless, we have recently demonstrated that intense SER spectra are obtained even for transition-metal hexaammine complexes that are electrostatically adsorbed at silver electrodes in halide media.⁹ Bands associated with both metal-ammine and internal ammine modes are observed.⁹ These conditions are similar to those employed here and indeed suggest that both adsorption and the consequent appearance of SER spectra of the nitrogen heterocycle complexes may be associated as much with strong electrostatic attraction of the multicharged cationic complexes to the specifically adsorbed halide anions as with surface binding of the heterocyclic ligands.^{8b}

Internal Pyridine Modes

Nearly all the remaining SER vibrational bands can be accounted for in terms of internal nitrogen heterocycle modes. The SERS vibrational mode assignments for the present pyridine and pyrazine complexes are aided considerably by the availability of detailed SERS studies of the adsorbed free ligands at silver electrodes.^{26,27} Summaries of representative SER spectra for free pyridine and pyrazine obtained in the present work are also given in Tables 2 and 4, respectively. A further aid to spectral assignments was provided by the influence of pyridine ring deuteration upon the SERS vibrational frequencies for $\text{Os}(\text{NH}_3)_5\text{py}$ (Table 1).

The 27 vibrational modes expected for pyridine, assuming C_{2v} symmetry, consist of $10A_1$, $3A_2$, $9B_1$, and $5B_2$ symmetry modes.^{15,27} All these modes are expected to be both Raman and IR active. Although there are three fewer vibrational modes predicted for pyridine than benzene, (those absent have Wilson mode numbers 7a, 9b, and 17b¹⁵), the lower molecular symmetry for pyridine lifts the degeneracy of the remaining modes, yielding more spectral peaks. Most of these modes are observed in the SER spectra of adsorbed pyridine; and as expected, bands arising from the A_1 modes are the most intense.²⁷ The frequencies are very close to those for bulk-phase aqueous pyridine.^{26,27} Bands corresponding to most of these modes are also seen in the SER spectra of $\text{Os}(\text{NH}_3)_5\text{py}$ and $\text{Ru}(\text{NH}_3)_5\text{py}$ (Tables 1 and 2). For free pyridine at silver the most prominent SERS bands occur at ca. 1007, 1035, 1216, and 1597 cm^{-1} , corresponding to the totally symmetric ring breathing mode (Wilson mode 1), the trigonal ring breathing mode (12), a symmetric in-plane C-H bending mode (9a), and another ring breathing mode (8a; Table 2). For SERS of $\text{Os}^{\text{III}}(\text{NH}_3)_5\text{py}$, these modes are observed at 1020, 1076, 1216, and 1592 cm^{-1} (Table 1). It is interesting to note that similar frequencies are seen for these modes in the

bulk-phase IR and normal Raman spectra, although the latter spectrum is relatively sparse.

Electroreduction of adsorbed $\text{Os}^{\text{III}}(\text{NH}_3)_5\text{py}$ to $\text{Os}^{\text{II}}(\text{NH}_3)_5\text{py}$ yields noticeable frequency decreases of the 1020 cm^{-1} band to 992 cm^{-1} and the 1076 cm^{-1} band to 1054 cm^{-1} , whereas the other two modes noted above remain relatively unaltered (Table 1). These frequency shifts can be understood in terms of the additional electron density expected on the pyridine ring when coordinated to Os(II) rather than Os(III).⁸ For $\text{Ru}^{\text{II}}(\text{NH}_3)_5\text{py}$, these four SERS bands occur at 1011 , 1054 , 1222 , and 1591 cm^{-1} (Table 2). The higher frequency of the first mode for Ru(II) relative to that for Os(II) is compatible with the smaller extent of metal-pyridine back bonding expected for the former complex.^{8b} Additional A_1 modes are observed in the SER spectra for these complexes at ca. 650 (6a), 1050 (18a), 2900 (13), and 3200 cm^{-1} (2). The opposite assignments are usually given for modes 12 and 18a. The present assignment is made, albeit tentatively, on the expectation that the more symmetrical trigonal ring breathing mode 12 will have a larger intensity as well as a greater sensitivity to the metal oxidation state.

Deuteration of the pyridine ring on $\text{Os}^{\text{III}}(\text{NH}_3)_5\text{py}$ and $\text{Os}^{\text{II}}(\text{NH}_3)_5\text{py}$ shifts the 6a, 1, 12, 18a, and 8a modes to lower frequencies by factors close to the ratio 0.97 observed for bulk-phase pyridine and metal pyridine complexes (Table 1);²⁸ such shifts are consistent with the assignment of these bands to ring modes.²⁸ The corresponding deuteration frequency ratios for the 12, 9a, and 13 modes were around 0.73, as expected for C-H modes, and again consistent with the effects of deuteration upon bulk-phase pyridine spectra.²⁸

Although pyridine deuteration shifts Wilson mode 2 for $\text{Os}^{\text{III}}(\text{NH}_3)_5\text{py}$ to around 2300 cm^{-1} , a smaller peak remains at 3200 cm^{-1} (Table 1). This is

most likely due to the N-H stretching mode appearing upon removal of the accidental degeneracy of these two modes (*vide supra*). The breadth of the latter adds to the difficulty in making distinct assignments in this frequency region. Thus although the 20a mode is also anticipated in this region, it is not observed and may be buried beneath stronger peaks. The assignment of the 2900 and 3200 cm^{-1} bands to modes 2 and 13 is based on their expected greater intensity.²⁷

Of the three predicted A_2 modes (10a, 16a, 17a), only the first is detected in the SER spectra, appearing for $\text{Ru}^{\text{II}}(\text{NH}_3)_5\text{py}$ at ca. 735 cm^{-1} (Table 2). Most of the nine B_1 modes can be accounted for in the present spectra. Peaks at ca. 1150, 1450 and 1575 cm^{-1} for pyridine on silver (Table 2) are similarly observed for the pyridine complexes and thus are assigned 9b, 19b and 8b, respectively. The 1150 cm^{-1} band for $\text{Os}(\text{NH}_3)_5\text{py}$ could alternatively be assigned to mode 15. The absence of the pyridine mode 6b for SERS of $\text{Os}(\text{NH}_3)_5\text{py}$ and $\text{Ru}(\text{NH}_3)_5\text{py}$ (Tables 1,2) may be due to accidental degeneracy with mode 6a. Since a large change in dipole moment and reduced symmetry will favor the appearance of modes 3, 7b and 20b to a greater extent in the IR than the NR spectra, it is not too surprising that they are not detected in the SER spectra. Their appearance in the IR spectra at ca. 1245, 2950, and 2980 cm^{-1} support these assignments. Mode 14 occurs in both the IR and SER spectra of $\text{Os}(\text{NH}_3)_5\text{py}$ at 1385 cm^{-1} and shifts as expected²⁸ to ca. 1320 cm^{-1} upon deuteration (Table 1).

The remaining 5 B_2 modes are all out-of-plane vibrations and are observed below 1000 cm^{-1} in the SER spectra of $\text{Os}(\text{NH}_3)_5\text{py}$. Some of these modes can be identified by comparison with the pyridine SER spectra. Thus the 415 cm^{-1} band for $\text{Os}(\text{NH}_3)_5\text{py}$ (Table 1) is close to the frequency expected for the pyridine ring mode 16b.²⁷ Indeed pyridine deuteration decreases the frequency

by the factor 0.92, in good agreement with that seen for pyridine and other pyridine complexes.²⁸ Further support to this assignment over the alternative designation as a metal-ammine vibration (*vide supra*) is given by the observed insensitivity of the frequency to the osmium oxidation state (Table 1).

Assignment of the band around 900 cm^{-1} for $\text{Os}(\text{NH}_3)_5\text{py}$ to the C-H stretch mode 10b is similarly supported by the frequency decrease by the factor 0.78 seen upon pyridine deuteration (Table 1). Modes 10a, 11 and 4 are expected to occur around 700 cm^{-1} .¹⁵ The latter two modes are expected to yield strong IR bands on the basis of their B_2 symmetry; they are thereby assigned to the bands at ca. 740 and 760 cm^{-1} , respectively for $\text{Os}(\text{NH}_3)_5\text{py}$ (Table 1).

In addition, several unassigned peaks are observed in the SER spectra, most notably at 1271 cm^{-1} for $\text{Os}(\text{NH}_3)_5\text{py}$, and 518 cm^{-1} and 1176 cm^{-1} for $\text{Ru}^{\text{II}}(\text{NH}_3)_5\text{py}$. These peaks may be due to combinations, overtones, Fermi resonance, or to adsorbed impurities.

Several general trends are apparent when viewing Tables 1 and 2. In particular, complexation of pyridine to osmium or ruthenium shifts several modes by $10\text{-}20\text{ cm}^{-1}$ to higher frequencies. A similar observation has also been made for other metal pyridine complexes, and attributed to coupling of the pyridine ring modes with the metal-ligand vibrations.^{21a} As noted above, similarly to the metal-ammine modes several of the pyridine modes shift significantly upon alteration of the metal oxidation state. However, it also should be noted that the frequencies of the SER spectra are not significantly shifted ($<5\text{ cm}^{-1}$) compared to the corresponding IR and normal Raman values for the complexes. This is indicative of only weak interactions between the adsorbed complexes and the silver surface.

Internal Pyrazine Modes

There are 24 predicted vibrational modes for pyrazine, consisting of $5A_g$, $1B_{1g}$, $4B_{2g}$, and $2B_{3g}$ Raman-allowed modes, $2A_u$ forbidden modes, and $4B_{1u}$, $2B_{2u}$, and $4B_{3u}$ infrared-allowed modes for D_{2h} symmetry (g: gerade; u: ungerade). Thus there are five fewer modes expected for pyrazine than pyridine; these are the two A_u modes (16a and 17a), one B_{3g} mode (10b), one B_{3u} mode (18b), and one B_{1u} mode (20a). Although the symmetrical nature of pyrazine makes the appearance of Raman and IR modes mutually exclusive, adsorption as well as metal coordination will relax this rule somewhat.³¹ Furthermore, the greater adsorbate-surface interactions expected to result from surface attachment of the remote pyrazine nitrogen may well shift the band frequencies and alter their relative intensities, making the assignments somewhat more tentative.

Again the most prominent modes in the normal Raman and SER spectra for $Os(NH_3)_5pz$ and $Ru(NH_3)_5pz$, as well as the SER spectra of free pyrazine, are the totally symmetric modes (A_g ; Tables 3 and 4). The observed frequencies at ca. 1020, 1230, and 1600 cm^{-1} for these complexes are assigned to modes 1, 9a and 8a, as deduced from the similar frequencies found for liquid pyrazine,¹⁵ pyrazine adsorbed at silver,²⁷ and bulk-phase metal pyrazine complexes.³⁰ The appearance of these modes for the complexes with considerable intensity in the IR spectra is indicative of selection rule breakdown.

The other two A_g mode assignments are not so clearcut. Several peaks appear between 600 and 750 cm^{-1} , where the 6a mode is expected along with modes 6b (B_{2g}) and 4 (B_{3g}). The lower two frequency peaks have been alternately assigned to modes 6a and 6b, while mode 4 is generally assigned to the highest frequency.^{15,27,31,32} Of these the most intense peak in the Raman spectra for

$\text{Os}(\text{NH}_3)_5\text{pz}$ and $\text{Ru}(\text{NH}_3)_5\text{pz}$ occurs at ca. 700 cm^{-1} and is therefore assigned to the A_g mode 6a. Modes 6b and 4 are then assigned to the $660-680 \text{ cm}^{-1}$ and ca. 735 cm^{-1} peaks, respectively.

The final A_g mode (2) is left unassigned; N-H stretching modes occur in the ca. 3100 cm^{-1} frequency region, where this band is expected (*vide supra*) (Table 3 and 4). Although a C-H stretching mode is observed for $\text{Ru}(\text{NH}_3)_5\text{pz}$ at 3010 cm^{-1} its frequency corresponds most closely to mode 7b (B_{2g}) for pyrazine at silver²⁷. Two other C-H stretching modes are seen for these complexes, but only in the IR spectra. They are assigned to the ungerade symmetry modes 13 (B_{1u}) and 20b (B_{3u}), on the basis of data for similar metal-pyrazine complexes.³⁰

Of the B_{1u} modes, only the trigonal ring breathing mode 12 is clearly detected in the SER spectra for $\text{Os}^{\text{III}}(\text{NH}_3)_5\text{pz}$ and $\text{Ru}^{\text{II}}(\text{NH}_3)_5\text{pz}$. Although mode 18a is expected at similar frequencies it may be hidden by the more intense mode 12. The remaining B_{1u} modes 13 and 19a are observed in the IR spectra as expected (Tables 3 and 4).

For the remaining symmetry species only a few modes [4 (*vide supra*), 10a, 11, 14 and 19b] show detectable SER bands. These modes were again assigned chiefly by comparison with previous analyses for bulk-phase and adsorbed pyrazine.²⁷ A number of additional bands are found in the IR spectra and are assigned based on symmetry arguments and comparison with literature assignments.³⁰ Several peaks at ca. 520, 1040 (Raman and IR only) and 1420 cm^{-1} for $\text{Os}(\text{NH}_3)_5\text{pz}$ and ca. 520, 1030, 1260 and 1420 cm^{-1} for $\text{Ru}(\text{NH}_3)_5\text{pz}$ remain unassigned, and again may be attributed to overtones, combinations or Fermi resonance.

Similar to the pyridine complexes, $\text{Os}(\text{NH}_3)_5\text{pz}$ and $\text{Ru}(\text{NH}_3)_5\text{pz}$ exhibit several bands having potential-dependent frequencies, in particular metal-ligand

mode I and pyrazine modes 1, 6a, and 12. However, as mentioned above these shifts are not wholly associated with an oxidation state change for the coordinating metals, especially since the formal potential for the Ru (III/II) couple is positive of the potential region studied.^{8b} These potential dependencies appear to be due in part to the involvement of different surface sites, molecular orientations, etc., possibly associated with specific interactions of the pyrazine ligand with the silver surface.^{8b}

Internal Bipyridine Modes

The $\text{Os}(\text{NH}_3)_5\text{bpy}$ SER spectra are necessarily more complicated, due to the increased number of vibrational modes. The measurements were limited to a relatively cursory study of the SERS of $\text{Os}(\text{NH}_3)_5\text{bpy}$ and bipyridine (Table 5). However, reasonable assignments can be ascertained if a flat molecule is assumed, i.e. the rings are contained in the same plane. The molecule then has D_{2h} symmetry with 54 predicted vibrations. Group symmetry arguments yield 10A_g 3B_{1g}, 9B_{2g} and 5B_{3g} Raman active modes, 4A_u forbidden modes and 9B_{1u}, 5B_{2u} and 9B_{3u} infrared active modes. Most of the observed modes can be assigned primarily by comparison with previous vibrational analyses of related molecules, especially biphenyl.³³

In group symmetry analyses the choice of axis labels is somewhat arbitrary. The x, y and z axis were chosen in the present study to be consistent with the above analysis of pyridine and pyrazine. The axis have therefore been interchanged with those employed for biphenyl such that the Wilson numbering scheme can be maintained.³³ Each pyridine mode is split into an in-phase and out-of-phase component for the bipyridine complex. Thus the pyridine A₁ modes become an A_g mode where the two ring motions are in-phase and a B_{1u} mode where the ring motions are out-of-phase. By analogy to biphenyl, the former modes are shifted to higher frequencies, whereas the latter

modes are unaffected and are comparable in frequency to the corresponding pyridine modes. Although extensive normal coordinate analysis has been carried out for only the in-plane biphenyl modes,³³ these constitute the majority of the experimentally observed modes. These include the A_g , B_{1u} , B_{2g} and B_{3u} modes.

Similarly to pyridine and pyrazine ligands, the most intense SERS bands for $Os(NH_3)_5bpy$ and bipyridine were found to be the symmetric in-phase stretching modes (A_g) (Table 5). The remaining A_g modes 2 and 13 occur in the high frequency region, but unfortunately these peaks were broad and weak and therefore are not reported in Table 5. The out-of-plane compliments to the A_g modes, the B_{1u} modes, also have significant intensity in the SER spectra. These modes are easily assigned by their nearly coincident frequencies with those for pyridine. Of the remaining eighteen in-plane modes only four (6b, 8b, 15, 18a) are observed for bipyridine and two (6b, 8b) for $Os(NH_3)_5bpy$ (Table 5). Since the in- and out-of-plane component of these modes are predicted to occur at approximately the same frequency and only one spectral peak appears, no phase assignment is made for modes 15 and 8b. Several out-of-plane modes also appear but are generally weak. Other bands due to out-of-plane modes are also anticipated to be relatively weak. Since they are expected to occur at similar frequencies to the in-plane modes, they may not be observed due to accidental degeneracy.

Additionally, two new modes occur in the spectra due to inter-ring stretching. Both are of A_g symmetry and are found at ca. 355 and 1295 cm^{-1} for bipyridine and ca. 1305 cm^{-1} for $Os(NH_3)_5bpy$. For the latter adsorbate the lower frequency mode may be hidden by the intense metal-ligand mode I (Table 5).

Viewing Table 5 reveals several general features. It is noticeably devoid of metal-ammine and other metal-ligand modes. This may be due to a reduced SER enhancement caused by the greater distance between the metal center and the electrode surface. The totally symmetric pyridine modes (A_1) are nearly all observed as pairs composed of in- and out-of-phase components although, the former modes are generally more intense. By analogy with the potential-dependent $Os(NH_3)_5py$ and $Os(NH_3)_5pz$ spectra, the appearance of the band at 996 cm^{-1} for $Os(NH_3)_5bpy$ as the potential is made more negative may be associated with the formation of the Os(II) oxidation state, as is the appearance of a lower frequency metal-ligand stretching mode under these conditions. Indeed, such a redox state change is consistent with the electrochemical data.^{8b} However, as for $Os(NH_3)_5pz$ the higher frequency band also survives at more negative potentials, suggesting that more than one type of adsorbate stereochemistry may be involved. However, the additional structural complexity of the bipyridine adsorbates render such interpretations somewhat speculative.

CONCLUSIONS

The intensity and richness of the present SER spectra, coupled with the need to employ only very small quantities of material, suggest that the technique may have wide utility for obtaining detailed vibrational information for coordination compounds that can be chemically or electrostatically adsorbed at metal surfaces. Indeed the signal intensities are commonly as great as those obtained for resonance Raman spectroscopy. Although the relaxation of selection rules for SERS yields more complete vibrational spectra, this makes the assignment of vibrational modes necessarily more complicated. Nevertheless, this can be minimized by careful comparisons with bulk NR and IR spectra. An additional important virtue of the SERS method is that it enables spectra to be obtained for species, such as Os(II), that are difficult to examine in

bulk media due to their chemical instability. Further applications of SERS for examining the molecular structural details of electrochemical redox processes involving coordination compounds at silver and gold electrodes are being pursued in this laboratory.

ACKNOWLEDGMENTS

PAL acknowledges a CSIRO postdoctoral fellowship, and MJW a fellowship from the Alfred P. Sloan Foundation. This work is supported in part by the Office of Naval Research and the Air Force Office of Scientific Research.

REFERENCES

- (1) For reviews see, (a) R.P. Van Duyne in "Chemical and Biochemical Applications of Lasers", Vol. 4, C.B. Moore (ed), Academic Press, N.Y., 1979, Chapter 5; (b) R.L. Burke, J.R. Lombardi, L.A. Sanchez, *Adv. Chem. Ser.*, 201, 69 (1982); (c) R.K. Chang, B.L. Laube, *CRC Crit. Rev. Solid State and Mat. Sci.*, in press.
- (2) H. Wetzel, H. Gerischer, B. Pettinger, *Chem. Phys. Lett.*, 78, 392 (1981); M. Fleischmann, P.J. Hendra, I.R. Hill, M.E. Pemble, *J. Electroanal. Chem.*, 117, 243 (1981).
- (3) H. Wetzel, H. Gerischer, B. Pettinger, *Chem. Phys. Lett.*, 80, 159 (1981). M.J. Weaver, F. Barz, J.G. Gordon II, M.R. Philpott, *Surf. Sci.*, 125, 409 (1983).
- (4) T.M. Cotton, S.G. Schultz, R.P. Van Duyne, *J. Am. Chem. Soc.*, 102, 7962 (1980).
- (5) For example, see A.B. Anderson, R. Kotz, E. Yeager, *Chem. Phys. Lett.*, 82, 130 (1981); M. Fleischmann, I.R. Hill, M.E. Pemble, *J. Electroanal. Chem.*, 136, 361 (1982).
- (6) (a) M.J. Weaver, J.T. Hupp, F. Barz, J. G. Gordon II, M.R. Philpott, *J. Electroanal. Chem.*, 160, 321 (1984); (b) J.T. Hupp, D. Larkin, M.J. Weaver, *Surf. Sci.* 125, 429 (1983).
- (7) J.E. Pemberton, R.P. Buck, *J. Phys. Chem.*, 85, 248 (1981).
- (8) (a) S. Farquharson, M.J. Weaver, P.A. Lay, R.H. Magnuson, H. Taube, *J. Am. Chem. Soc.*, 105, 3350 (1983); (b) S. Farquharson, K.L. Guyer, P.A. Lay, R.H. Magnuson, M.J. Weaver, *J. Am. Chem. Soc.*, in press.
- (9) M.A. Tadayyon, S. Farquharson, M.J. Weaver, *J. Chem. Phys.* 80, 1363 (1984).
- (10) M.A. Tadayyon, S. Farquharson, T.T-T. Li, M.J. Weaver, *J. Phys. Chem.*, in press.
- (11) S. Farquharson, D. Milner, M.A. Tadayyon, M.J. Weaver, *J. Electroanal. Chem.*, in press.
- (12) (a) P.A. Lay, R.H. Magnuson, J. Sen, H. Taube, *J. Am. Chem. Soc.*, 104, 7658 (1982); (b) P. Ford, D.P. Rudd, R. Gaunder, H. Taube, *J. Am. Chem. Soc.*, 90, 1187 (1967).
- (13) D.P. Rudd, H. Taube, *Inorg. Chem.*, 10, 1543 (1971); P.A. Lay, R.H. Magnuson, H. Taube, to be published.
- (14) K.L. Guyer, Ph.D. thesis, Michigan State University, 1981.
- (15) (a) R.C. Lord, A.L. Marston, F.A. Miller, *Spectrochim. Acta* 9, 113 (1957); (b) E.B. Wilson, *Phys. Rev.*, 45, 706 (1934).
- (16) K.H. Schmidt, A. Müller, *Coord. Chem. Rev.*, 19, 41 (1976).

- (17) M.W. Bee, S.F.A. Kettle, D.B. Powell, *Spectrochim. Acta.* 30A, 139 (1974); A.D. Allen, C.V. Senoff, *Can. J. Chem.*, 45, 1337 (1967).
- (18) K. Nakamoto, "Infrared and Raman Spectra of Inorganic and Coordination Compounds", Wiley, New York, 1978, 3rd edition, p. 161.
- (19) Ref. 18, pp. 197-323.
- (20) R. Dornhaus, R.K. Chang, *Solid State Comm.*, 34, 811 (1980); H. Wetzel, H. Gerischer, B. Pettinger, *Chem. Phys. Lett.*, 78, 392 (1981).
- (21) (a) R.J.H. Clark, C.S. Williams, *Inorg. Chem.*, 4, 350 (1965);
(b) M. Choca, J.R. Ferraro, K. Nakamoto, *J. Chem. Soc. Dalton*, 2297 (1972);
(c) S. Akyuz, A.B. Dempster, R.L. Morehouse, S. Suzuki, *J. Mol. Struct.*, 17, 105 (1973); (d) C.D. Flint, A.P. Matthews, *Inorg. Chem.*, 14, 1008 (1975).
- (22) M.D. Child, G.A. Foulds, G.C. Percy, D.A. Thornton, *J. Mol. Struct.*, 75, 191 (1981).
- (23) T.C. Strekas, T.G. Spiro, *Inorg. Chem.*, 15, 974 (1976).
- (24) H.E. Toma, P.S. Santos, *Can. J. Chem.*, 55, 3549 (1977)
- (25) J.A. Chambers, R.P. Buck, *J. Electroanal. Chem.*, in press.
- (26) D.L. Jeanmaire, R.P. Van Duyne, *J. Electroanal. Chem.*, 84, 1 (1977).
- (27) R. Dornhaus, M.B. Long, R.E. Benner, R.K. Chang, *Surf. Sci.*, 93, 240 (1980).
- (28) G.A. Foulds, J.B. Hodgson, A.T. Hutton, M.L. Nevin, G.C. Percy, P.E. Rutherford, D.A. Thornton, *Spect. Lett.*, 12, 25 (1979).
- (29) M. Moskovits, *J. Chem. Phys.*, 77, 4408 (1982).
- (30) M. Goldstein, W.D. Unsworth, *Spectrochim. Acta.*, 27A, 1055 (1971).
- (31) L.M. Sverdlov, M.A. Kovner, E.P. Krainov, "Vibrational Spectra of Polyatomic Molecules", Wiley, New York, 1974.
- (32) J.D. Simmons, K.K. Innes, *J. Mol. Spect.*, 14, 190 (1964).
- (33) G. Zerbi, S. Sandroni, *Spectrochim. Acta.* 24A, 483, 511 (1968).

Table 1. Summary of SER spectra for $\text{Os}(\text{NH}_3)_5\text{py}(1\text{I}), (1\text{I})$; effects of pyridine ring and ammine deuteration, and comparison with normal Raman and infrared spectra.

Mode Number ^a	Symmetry Species ^b	Brief Vibrational Description	IR ^{c,e,f,h}			Raman ^{e,f}			SERS			
			Os(1I)	Os(1I)	Os(1I)	-150 mV	-750 mV	-150 mV	-750 mV	-150 mV	-750 mV	ND ₃ ^m
I A ₁	$\nu_{\text{M}-\text{N}}$						267s		263m			256s
16b B ₂	γ_{ring} u	444m				415w	417w	381m	384w			
VIII E	$\nu_{\text{M}-\text{N}}$	466m										
XI E	$\nu_{\text{M}-\text{N}}$					494w	468m	480m	460m,br	461m		436m
II A ₁	$\nu_{\text{M}-\text{N}}$ u	520s		501w								
III A ₁	$\nu_{\text{M}-\text{N}}$					573w,br	557m,br					
6a A ₁	δ_{ring}	649w		654m	654m	648s	623w	618m	655m	647m		
11 B ₂	$\gamma_{\text{C}-\text{H}}$	696vs		704m			739w			701m	698w	
4 B ₂	$\gamma_{\text{C}-\text{H}}$	760vs					765w					
10a A ₁	$\gamma_{\text{C}-\text{H}}$	790m					807w					
E	δ_{NH_3} (rock)	851vs,br										
10b B ₂	$\gamma_{\text{C}-\text{H}}$				895w	900m		702m			898w	
5 B ₂	γ_{ring}	955w				960w		797w				
1 A ₁	ν_{ring}	1022m	990m	1020s	1020vs	992s	978vs	955s	1019vs	989s		
18a A ₁	$\delta_{\text{C}-\text{H}}$	1055vw				1050w		1022w				
12 A ₁	ν_{ring}	1074s	1055w			1076m	1054s	1042m,sh	1025m	1078m	1054m	
9b/15B ₁	$\delta_{\text{C}-\text{H}}$	1157m		1154vw	1151w	1151w						
9a A ₁	$\delta_{\text{C}-\text{H}}$	1216m,br		1221m	1216m,br	1210s			896m	1220s	1210s	
3 B ₁	$\delta_{\text{C}-\text{H}}$ u	1241w				1271m		1234m		1267w		
E	δ_{NH_3} (sv)	1347vs				1354m	1254w,sh			1085m,sh		
14 B ₁	$\delta_{\text{C}-\text{H}}$	1373s,sh				1386s	1385w	1322vs	1325m	1321s		
19b B ₁	ν_{ring}	1442vs				1441w	1430w,br				1443w	
19a A ₁	ν_{ring}	1494s										
8b B ₁	$\delta_{\text{C}-\text{H}}$	1584s,sh										
8a A ₁	$\delta_{\text{C}-\text{H}}$			1600m,sh	1592vs,br	1593s	1552vs	1550s	160vs,br	1593vs		
E	δ_{NH_3} (as)	1608vs		1613s	1620s,br		1604vs	1600m,br	1170s			
13 A ₁	$\nu_{\text{C}-\text{H}}$				2900w,br	2910w,br		2100m,br				
7b B ₁	$\nu_{\text{C}-\text{H}}$	2940m							2930s	2920m,br		
2 A ₁	$\nu_{\text{C}-\text{H}}$				3200m,br	3210m,br	2310m					
A ₁	ν_{NH_3}	3150vs,br			3200m,br	3210m,br	3220s,br	3230s,br				

Table 2. Symmetry species, vibrational assignments, and infrared spectra for $\text{Ru}(\text{NH}_3)_5\text{py}$ (II), (II), and SERS and Raman spectra for $\text{Ru}(\text{NH}_3)_5\text{py}$ (II), (II), and SERS for the $\text{Ru}(\text{NH}_3)_5\text{py}$ complex in pyridine.

Mode Number ^a	Symmetry Species ^b	Brief Vibrational Description	$\text{Ru}(\text{NH}_3)_5\text{py}$						pyridine ^k	
			IR ^{c,g}		Raman ^{c,g}		SERS		SERS	
			Ru(III)	Ru(II)	Ru(III)	Ru(II)	-150 mV	-450 mV	-150 mV	-650 mV
I A ₁	$\nu_{\text{N}-\text{N}^+}$						303vs	297s		
16b B ₂	δ_{ring}	413vw					419vw,br	416vw	412vw	
VIII E	$\nu_{\text{M}-\text{N}_2^+}$	464s	450w	465m				456vw		
XI E	$\nu_{\text{M}-\text{N}_3^+}$	482m,sh	470w							
11 A ₁	$\nu_{\text{M}-\text{N}_4^+}$	496m,sh	498w	494m			518m	517w		
6a A ₁	δ_{ring}	648m	640w	646m	646m	654vs	655s	625w	627w	
6b B ₁	δ_{ring}							651vw	654w	
11 B ₂	$\tau_{\text{C}-\text{H}}$	703vs	693m			683s	682m			
10c A ₁	$\tau_{\text{C}-\text{H}}$					736m	734w			
4 B ₂	$\gamma_{\text{C}-\text{H}}$	777vs	770m					755w,br	757w,br	
E	ν_{NH_3} (rock)	825vs,br	815s,br			816m	817m			
10b B ₂	$\tau_{\text{C}-\text{H}}$	894w						880vw,br	875vw,br	
5 B ₂	γ_{ring}					959w,br		943vw	943vw	
1 A ₁	τ_{ring}	1017s	998s	1023s	1011s	1011s	1012s	1007vs	1006s	
12 A ₁	ν_{ring}	1069s	1050m		1057w	1054s	1054s	1037s	1034s	
18a A ₁	$\delta_{\text{C}-\text{H}}$	1050w						1067w	1065s	
15 B ₁	$\delta_{\text{C}-\text{H}}$	1153m,sh	1150w				1144vw	1154vw	1153vw	
4b B ₁	$\delta_{\text{C}-\text{H}}$	1176s	1176m							
9a A ₁	$\delta_{\text{C}-\text{H}}$	1223m		1218s	1217s	1222vs	1222s	1216m	1216m	
3 B ₁	$\delta_{\text{C}-\text{H}}$	1245m								
		1292s								
F	δ_{NH_3} (sy)	1325vs				1260m				
		1356s	1328m			1360m,br	1368vw,br			
14 B ₁	$\delta_{\text{C}-\text{H}}$	1393s	1390m					1445vw		
19b B ₁	ν_{ring}	1446vs	1446s			1468m	1468m		1487vw	1482vw
19a A ₁	ν_{ring}	1493vs	1490m						1573w	1573w,sh
8b B ₁	$\delta_{\text{C}-\text{H}}$			1602s	1606s	1601s	1591vs	1591s	1597m	1597s
8a A ₁	$\delta_{\text{C}-\text{H}}$		1609vs	1610s,br		1611vw				
E	δ_{NH_3} (as)									
7b B ₁	$\nu_{\text{C}-\text{H}}$	2951s,sh	2940s,sh							
20a B ₁	$\nu_{\text{C}-\text{H}}$	2981s,sh	2980w							
2 A ₁	$\nu_{\text{C}-\text{H}}$							3060s,br	3050s,br	
F ₁	$\nu_{\text{N}-\text{H}}$ (sy)	3140vs,br	3115m,sh							
A ₁	$\nu_{\text{N}-\text{H}}$ (as)		3200s,br							

Table 3. Summary of SIR, Raman, and infrared spectra for $\text{Os}(\text{NH}_3)_5\text{pz}(\text{II}), (\text{II})$; effect of aqueous deuteration.

Mode Number ^a	Symmetry Species ^b	Brief vibrational description	IR ^c		Raman ^d		SERS			
			Os(III)	Os(II)	Os(III)	Os(II)	-150 mV	-550 mV	-150 mV	-550 mV
I	A_1	$\nu_{\text{M}-\text{N}}$			350vw	287s	345vs	304vs 343s	345vs	299vs 340s
VIII	E	$\nu_{\text{M}-\text{N}}$		450m			461w	440vw		
16b	B_{2u}	γ_{ring}					494w	496w	487w	487w
III	A_1	$\nu_{\text{M}-\text{N}}$	557m							
6b	B_{2g}	δ_{ring}	684m		658m	662m				
6a	A_g	δ_{ring}		700s	710s	707s	702s	673vs 699m	701s	670vs 700m
4	B_{3g}	$\gamma_{\text{C}-\text{H}}$					736m	736w		739w
10a	B_{1g}	$\gamma_{\text{C}-\text{H}}$		771m				762w		
11	B_{2u}	γ_{ring}	816w,sh				820vw	814w	816w	807m
	E	ρ_{NH_3} (rock)	848s		810s					
5	B_{3g}	γ_{ring}	874s							
1	A_g	ν_{ring}	1022m	1000s	1021m	988m	1020s	985m 1020m	1019s	991m 1020m
	u		1040m	1034s		1045w				
12	B_{1u}	ν_{ring}	1091m	1067s			1070m	1067vs 1088m,sh	1070m,sh 1089s	1066vs 1087m,sh
15	B_{3u}	$\delta_{\text{C}-\text{H}}$	1157s		1162s					
9a	A_g	$\delta_{\text{C}-\text{H}}$	1251m	1232m	1236m	1240m	1232s	1223m	1230s	1224s
	E	δ_{NH_3} (sy)	1339m,sh	1355s	1263vs					
14	B_{3u}	$\delta_{\text{C}-\text{H}}$	1425m	1415m	1416vw	1417vw	1365vw	1366m		1318vw
19b	B_{3u}	ν_{ring}	1441m	1445s			1464m	1464s	1464s	1464s
19a	B_{1u}	ν_{ring}	1497w	1490m						
8b	B_{2g}	$\delta_{\text{C}-\text{H}}$	1592s,sh		1586m,sh					
8a	A_g	$\delta_{\text{C}-\text{H}}$		1608s,sh	1603m	1601s	1602s	1590m	1600s	1594s
	E	δ_{NH_3} (as)	1606s,br	1616s	1614w					2925m
20b	B_{3u}	$\nu_{\text{C}-\text{H}}$	2978m	2979m						
7b	B_{2g}	$\nu_{\text{C}-\text{H}}$	3022s							
13	B_{1u}	$\nu_{\text{C}-\text{H}}$	3075s							
	A_1	$\nu_{\text{N}-\text{H}}(\text{sy})$			3119s,sh					
	A_1	$\nu_{\text{N}-\text{H}}(\text{as})$	3220s,br	3201s,br			3230w,br	3220m,br		

Table 4. Summary of SER, Raman, and infrared spectra for $\text{Ru}(\text{NH}_3)_5\text{pz}(\text{II})$; comparison with SER spectra for pyrazine.

Mode Number ^a	Symmetry Species ^b	Brief Vibrational Description	$\text{Ru}(\text{NH}_3)_5\text{pz}$			pyrazine ^k			
			IR ^{e,f}	Raman ^{e,i}	SERS		SERS		
					Ru(II)	-50 mV	-650 mV	-150 mV	-650 mV
1 A ₁	$\nu_{\text{M}-\text{N}}$		327vw	325s,br	302s,br				
10a A _u	γ_{ring}		377w				354w		
VIII E	$\nu_{\text{M}-\text{N}}$		456w	451vw	455vw				
XI E	$\nu_{\text{M}-\text{N}}$		472w						
16b B _{2u}	γ_{ring}		504w				441m	434m	
	u				524m	522m			
III A ₁	$\nu_{\text{M}-\text{N}}$			556w	568w				
6a A _g	δ_{ring}			692m	687s	675s	639s	636s	
6b B _{2g}	δ_{ring}		640s			642m	674m,sh	660m,sh	
					736m	735m	699m	699m	
10a B _{1g}	$\gamma_{\text{C-H}}$		753sh,br				742m	744m	
			780s						
11 B _{2u}	$\gamma_{\text{C-H}}$				820m	819m	806m	812m,br	
							898vw		
12 B _{1u}	γ_{ring}			1013m	1019m	1019s	1016s	1020s	1021s
				1030w				1050w	
12 B _{1u}	ν_{ring}				1076m,br	1077s	1056m,sh	1088m	
							1074m		
18a B _{1u}	$\delta_{\text{C-H}}$		1107w		1102w,sh	1101m,sh	1124w	1110w	
			1153w		1152w	1149vw	1160vw	1160vw	
15 B _{3u}	$\delta_{\text{C-H}}$				1190w	1190vw			
9b B _{2u}	$\delta_{\text{C-H}}$		1170w						
9a A _g	$\delta_{\text{C-H}}$		1221s	1229s	1227vs	1223s	1225s	1225s	
	u				1268m	1260m	1246m,sh		
			1295s						
13 B _{3u}	$\delta_{\text{N-H}}$ (sv)		1316s		1339w				
			1348s						
14 B _{3u}	$\delta_{\text{C-H}}$		1386w		1383w		1361w,br	1360w,br	
	u		1420s		1426w	1419w			
16b B _{3u}	γ_{ring}		1467m		1472m	1471m	1464w	1467w	
19a B _{1u}	ν_{ring}		1480m				1479w	1479w	
8b B _{2g}	$\delta_{\text{C-H}}$				1565m,sh	1563m,sh	1519m	1521m	
8a A _g	$\delta_{\text{C-H}}$		1579s	1601s	1593vs	1591s	1590vs	1588vs	
					1620s,br				
20b B _{1u}	$\epsilon_{\text{N-H}}$		2961m,br						
7b B _{2u}	$\nu_{\text{C-H}}$					3010w,br		3030w,br	
13 B _{3u}	$\nu_{\text{C-H}}$							3050w,br	
1 A ₁	$\nu_{\text{N-H}}$ (as)		3140s,br						
2 A ₁	$\nu_{\text{C-H}}$						3175w,br		
1 A ₁	$\nu_{\text{C-H}}$ (sv)		3282s,br						

Table 5. Summary of SERS spectra for $\text{Os}(\text{NH}_3)_5\text{bpy}$ (II), (II) and 4,4'-bipyridine.

Mode Number ^a	Symmetry Species ^b	Phase ^d	Brief Vibrational Description ^c	$\text{Os}(\text{NH}_3)_5\text{bpy}$		bipyridine ^k	
				SERS		SERS	
				-150 mV	-850 mV	-150 mV	-650 mV
							355vw
I	A_g		$\nu_{\text{r-r}}$				
16a	A_u	i	γ_{ring}	388vs,br	368m 397s	390m	386m
16b	B_{2u}	i	γ_{ring}			530m	497vw
6a	B_{1u}	o	δ_{ring}	636vs	637m	625m	
6b	B_{2g}	i	δ_{ring}	655w	651m	674w	666w
6a	A_g	i	δ_{ring}	770s	769s	767m	771s
11	B_{2u}	o	$\gamma_{\text{C-H}}$				806vw
10b	B_{3g}	o	$\gamma_{\text{C-H}}$				866w
5	B_{3g}	o	γ_{ring}			938m	942w
1	B_{1u}	o	ν_{ring}		996s	1004vs	
1	A_g	i	ν_{ring}	1005vs	1010s		1014vs
				1021m,sh	1024w,sh		
12	B_{1u}	o	ν_{ring}				1045w
12	A_g	i	ν_{ring}	1057vs	1053s	1058m	
18a	B_{3u}	i	$\delta_{\text{C-H}}$				1078m
15	B_{3u}	i	$\delta_{\text{C-H}}$			1141vw	1140m
9a	B_{1u}	o	$\delta_{\text{C-H}}$	1209vs	1210m,sh	1197m,sh	
9a	A_g	i	$\delta_{\text{C-H}}$	1228s,sh	1224s	1218s,br	1224s,br
	A_g		$\nu_{\text{r-r}}$	1305s	1301m,br	1296s	1295vs
						1334s	
19a	B_{1u}	o	ν_{ring}	1481m	1475m		
19a	A_g	i	ν_{ring}	1520s	1511m,br	1507s,sh	1516s
8b			$\delta_{\text{C-H}}$	1580s	1587vs	1558vs	
8a	B_{1u}	o	$\delta_{\text{C-H}}$	1603vs	1604s	1593vs	1606vs
8a	A_g	i	$\delta_{\text{C-H}}$	1628vs	1628s,sh	1634vs	1630s,sh

Footnotes to Tables 1-5.

Frequencies listed are typically accurate to within 2-3 cm^{-1} .
Explanation of symbols: w = weak, m = medium, s = strong, vs = very strong,
br = broad, sh = shoulder.

^aArabic numerals are Wilson numbers as assigned for benzene.

^bAssuming C_{2v} symmetry for nitrogen heterocycles; C_{4v} symmetry for metal-nitrogen modes.

^cVibrational assignments; see text for details. Symbols: ν , stretching mode;
 δ , in-plane bending mode; γ , out-of-plane bending mode; rock = rocking
mode; sy = symmetric; as = asymmetric; u = unassigned band.

^di = in-phase vibrations; o = out-of-plane vibrations.

^eBulk Raman spectra recorded as 1:1 mixture of Cl^- , ClO_4^- , I^- , or PF_6^-
salt to KBr or CsI in solid pellet.

^fchloride salt

^gperchlorate salt

^hiodide salt

ⁱhexfluorophosphate salt

^jSER spectra obtained using ca 0.1 - 1 mM complex at roughened silver
electrode in either 0.1 M NaBr- or 0.1 M NaCl - based electrolyte (see
text for details). For pyridine complexes, electrolyte also contained
0.1 M HCl to suppress hydrolysis. Electrode potentials quoted versus
saturated calomel electrode (sce).

^kSolution contained 10 mM pyridine; 1 mM pyrazine, or 1 mM 4,4'-bipyridine
in 0.1 M NaCl.

^lSER spectra for complex containing pentadeuterated pyridine.

^mSER spectra for complex containing deuterated ammine ligands;
prepared by dissolving complex in neutral D_2O before adding acidified
supporting electrolyte.

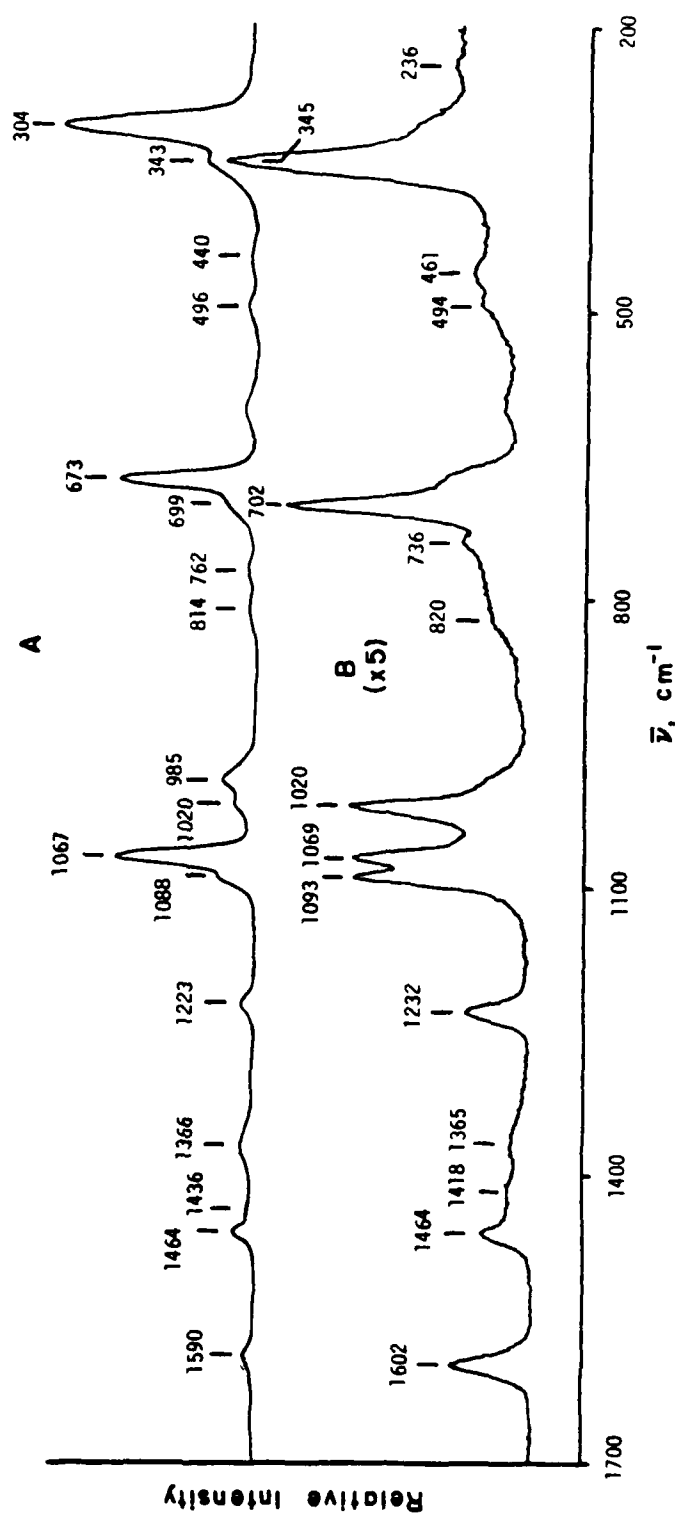


Figure Caption

SER spectra in $200\text{-}1700\text{ cm}^{-1}$ region for $\text{Os}(\text{NH}_3)_5\text{pz}$ at silver-aqueous interface following oxidation-reduction cycle at (A) -550 mV. (B) -150 mV vs. sce. Solution contained 0.1 mM $\text{Os}(\text{NH}_3)_5\text{pz}^{3+}$ in 0.1 M NaCl. Spectral conditions: 514.5 nm excitation, 100 mW incident power, scan speed $1\text{ cm}^{-1}\text{ sec}^{-1}$, time constant 1 sec, resolution 4 cm^{-1} . Note that spectra A is not smoothed, i.e. actual noise level is as shown.

EN

FILED